Lattice effects observed by the isotope-difference pair density function of the $YBa_2{}^{63/65}Cu_3O_{6.92}$ superconductor

Despina Louca and G. H. Kwei
Los Alamos National Laboratory, Los Alamos, New Mexico 87545

B. Dabrowski and Z. Bukowski
Department of Physics, Northern Illinois University, DeKalb, Illinois 60115

(Received 6 May 1999)

The local lattice effects in the $YBa_2Cu_3O_{6.92}$ superconductor were characterized by the neutron differential pair density function (DPDF) analysis. The DPDF provides an atom specific PDF, enabling the distinction between overlapping atom pair correlations in complicated systems. It utilizes the contrast in the scattering amplitude enhanced by the different neutron scattering lengths for ^{63}Cu and ^{65}Cu in two isotopically pure samples with identical compositions. Significant structural distortions are observed in the superconducting planes, in association with the plane copper (Cu2). A bifurcation of the Cu2 to apical oxygen (O4) pair correlations is evident which is temperature dependent. This effect originates from distortions along the *c* axis of the crystal of the Cu2 ions and not of the O4, as no distortions are observed in association with the connecting pair, the Cu1 (chain)-O4. Secondary lattice anharmonicities in the chains are also seen, arising mostly from defects in the vicinity of oxygen vacancies. [S0163-1829(99)12833-9]

I. INTRODUCTION

The normal and superconducting state properties of the $YBa_2Cu_3O_{7-\delta}$ (YBCO) high-temperature superconductor (HTSC) have been extensively studied[1] and the average crystallographic structure has been well characterized.[2] While at present it appears that most of the structural mysteries have been resolved, a controversy which started about a decade ago still endures. In particular, short range atomic structural distortions commonly characterized in the form of deviations from the long range symmetry describing the crystal might be present in this system, and in turn play a role in the mechanism for superconductivity. A precise definition of the type of distortions would in turn lead to a clear characterization of the role of lattice effects in this class of oxides. A way of identifying such atomic deviations from their ideal sites is through the use of a local structural probe where the constraints of lattice periodicity is not inherent in the analysis. It was thus suggested[3–6] using the x-ray-absorbtion fine-structure (XAFS) technique, a local probe, that bifurcation of the coupling of the chain copper to the apical oxygen atoms through a dynamic double well potential is triggered at temperatures well into the superconducting state and into the normal state. This subsequently led to the conclusion that such a motion is instigated as a consequence of the charge transfer from the donor chains to the superconducting planes. At the same time, contradictory results have been published.[7–10] Consequently, the uncertainty on the true nature of the distortions, if any, still remains.

The parent compound $YBa_2Cu_3O_6$ is an antiferromagnetic insulator with no oxygen atoms in the chains of the crystal.[11] A superconducting transition is observed with doping, for compositions with an oxygen content of 6.5 and higher. Above this value, the superconducting transition temperature, T_C, varies as a function of the oxygen defect content,[12] but does not exhibit a proportional relation to the amount of oxygen added in the chains. Optimally doped samples with $\delta \approx 0.05$ usually exhibit the highest T_C. For values smaller than that, T_C shows a decrease. The oxygen vacancies are more likely to form in the chains instead of the superconducting planes.[13] Whether they occupy sites at random or in order depends on the sample's preparation history and this becomes an important issue for samples with chain oxygen concentration close to half filling.[14] Thus, in the YBCO system, the lattice plays a significant role at least in the mechanism for changing T_C.

While lattice distortions have been observed in several HTSC materials (see Ref. 15 for review), they are not necessarily associated with an apical oxygen, if it is present at all in the structure. Previous neutron pair density function (PDF) studies provided evidence for local lattice distortions in several classes of superconducting materials.[16–19] In particular, in the thallium based compounds, Egami and coworkers showed that displacements of as large as 0.2–0.3 Å of the oxygen around the copper atoms occur in the local structure. For the optimally doped YBCO, however,[19] it has been quite difficult to concur on the presence or absence of such local lattice anharmonicities via PDF. Already the average crystal structure provides a good description for the local atomic structure. However, the complexity of the crystal structure allows for several pairs of atoms to have overlapping bond distance correlations in a reduced dimensional function such as the PDF, where due to the angular averaging, all information with regard to orientation is lost. This makes the resolution of the copper-oxygen pair correlations and any distortions associated with them practically impossible from other pairs, i.e., Y-O, Ba-O, O-O.

We implemented the isotope difference pair density function (DPDF) analysis. We investigated two optimally doped samples, made of isotopically pure ^{65}Cu and ^{63}Cu elements. Using the difference in the neutron scattering lengths of the two copper isotopes, a DPDF with respect to copper was

obtained which is analogous to an XAFS measurement performed at the Cu absorption edge. The advantage of the neutron DPDF, however, is that it has greater resolution. A quite pronounced distortion in association with the planar copper-apical oxygen pair is observed, which is manifested as a split in the bond to two. While this split shifts with temperature, it is consistently present in the local atomic structural state in the vicinity of T_C. This distortion originates primarily from motion of the planar copper and not of the oxygen atoms, along the *c* axis of the crystal. The analysis additionally concurs that the probability of a chain copper-apical oxygen interatomic distance with a separation of 0.135 Å is actually very small. Secondary lattice effects other than the planar copper distortions arise from chain defects and buckling of the planes.

II. SAMPLE PREPARATION AND DATA ANALYSIS

Polycrystalline samples of $YBa_2{}^{63}Cu_3O_7$ and $YBa_2{}^{65}Cu_3O_7$ (about 15 g each) were synthesized from stoichiometric mixtures of Y_2O_3, $BaCO_3$, ^{63}CuO, and ^{65}Cu using a wet-chemistry method. Weighed powders were dissolved in nitric acid at room temperature. Ammonium hydroxide and citric acid were added to obtain a complex citrate solution with pH$\sim$5. The solution was dried at 200–300 °C and decomposed in air at 500–600 °C. Sintering was done in air at 850 °C. Samples were pressed into pellets and fired in flowing oxygen at 950 °C followed by fast cooling to room temperature. Annealing was done in oxygen at 400 °C for two days. The wet-chemistry method leads to dense samples with homogeneous mixing of metal ions. The purity of the samples was checked by powder x-ray diffraction at room temperature. Both samples showed clean x-ray diffraction patterns with sharp peaks corresponding to the expected orthorhombic structure. The susceptibility measurements were performed with a Quantum Design Physical Properties Measurement System using ac magnetic fields at 20 Oe and 200 Hz. The resistivity was measured using standard four-leads dc method in zero applied field on cut bars with approximate dimensions $10\times2\times1$ mm. Both samples exhibit a superconducting transition at $T_C=92.5$ K, determined from the magnetic susceptibility χ and resistance measurements performed for each sample [Figs. 1(a) and 1(b)].

The experiments were performed at the Intense Pulsed Neutron Source (IPNS) of the Argonne National Laboratory using the Glass, Liquids and Amorphous materials Diffractometer (GLAD) and data were collected at temperatures close to and at the transition for a total of 12 h per temperature point per sample. The structure function $S(Q)$ determined from the diffraction pattern was normalized by the neutron scattering lengths for ^{63}Cu ($b=6.43$ fm) and ^{65}Cu ($b=10.61$ fm).[20] For a multicomponent system, the total dynamic structure factor is given by the following expression:

$$S(Q,\omega)=\sum_{\alpha} c_{\alpha}\overline{b_{\alpha}^2}S_{\alpha}(Q,\omega)+\sum_{\alpha,\beta} c_{\alpha}\overline{b_{\alpha}}c_{\beta}\overline{b_{\beta}}S_{\alpha,\beta}(Q,\omega) \tag{1}$$

with c_α as the atomic fraction, b_α as the neutron scattering length, and the bars indicating averages over the spin and isotope states of each element. The first and second terms are due to self- and interference scattering, respectively.

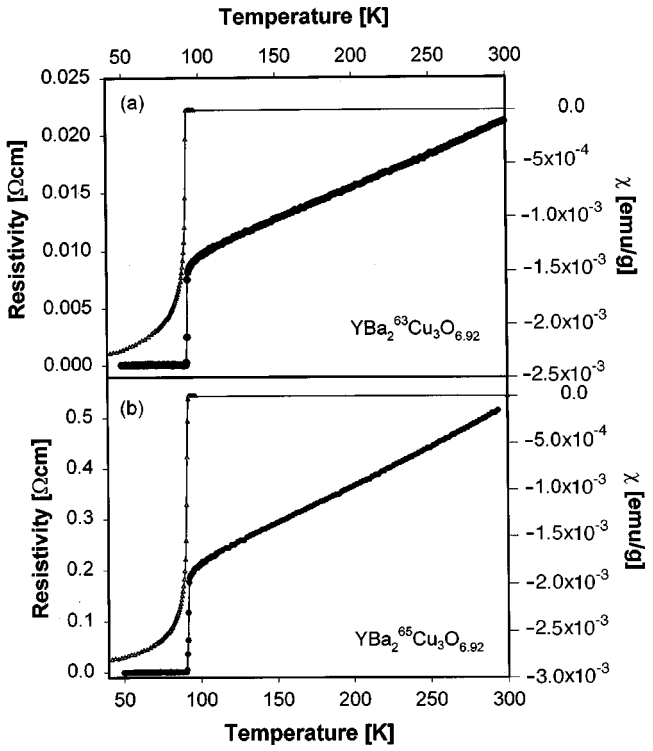

FIG. 1. The resistance and magnetic susceptibility χ plots of (a) the ^{63}Cu-YBCO and (b) the ^{65}Cu-YBCO compounds. The T_c of each sample is at 92.5 K.

The PDF $\rho(r)$ is a real space representation of atomic correlations obtained through a Fourier transformation of the $S(Q)$ (Ref. 21) where the $S(Q)$ is an integral over energy:[22,23]

$$S(Q)=S[Q(\omega=0)]=\int_{-\infty}^{\infty} S[Q(\omega),\omega]d\omega, \tag{2}$$

$$\rho(r)=\rho_0+\frac{1}{2\pi^2 r}\int_0^{Q_{\max}} Q[S(Q)-1]\sin(Qr)dQ. \tag{3}$$

The PDF's of the two isotopic samples were processed under identical conditions using the same termination $Q_{\max}$ point as well as the same background subtraction. The highest $Q_{\max}$ used in the analysis was 35 Å^{-1}. Subtraction of $\rho(r)$ of one isotopic material from the other at constant temperature provides the difference PDF (DPDF) with respect to Cu alone.[24] It is normalized by the corresponding average scattering lengths $\langle b\rangle$ so that the true intensity is recovered and the difference in the peak amplitude is only due to the difference in the neutron scattering amplitude for Cu:

$$\mathrm{DPDF}(T=\mathrm{const})=[\langle \mathbf{b}_{\mathrm{Cu}^{65}}\rangle^2\rho(\mathbf{r})_{\mathrm{Cu}^{65}}-\langle \mathbf{b}_{\mathrm{Cu}^{63}}\rangle^2\rho(\mathbf{r})_{\mathrm{Cu}^{63}}]. \tag{4}$$

Any pair that does not include the copper atom will be subtracted out. The resulting DPDF provides the local atomic structure with respect to Cu. This allows us to trace the temperature dependence of the copper to oxygen distances without obscuring the peaks that include this pair with other undesirable pair correlations such as from Ba-O and Y-O that have similar bond distances in the crystal structure. The sub-

TABLE I. The results of the Rietveld refinement of the neutron diffraction patterns for the positions of the atoms in the average crystallographic structure and atomic occupancy for the two $YBa_2^{63/65}Cu_3O_{7-\delta}$ isotopes.

	$YBa_2^{63}Cu_3O_{7-\delta}$		$YBa_2^{65}Cu_3O_{7-\delta}$	
Atom	Position	Occupancy	Position	Occupancy
Y	$\frac{1}{2}, \frac{1}{2}, \frac{1}{2}$	0.998	$\frac{1}{2}, \frac{1}{2}, \frac{1}{2}$	1.006
Ba	$\frac{1}{2}, \frac{1}{2}$, 0.1846	1.001	$\frac{1}{2}, \frac{1}{2}$, 0.1844	1.002
O1	0, $\frac{1}{2}$, 0	0.928	0, $\frac{1}{2}$, 0	0.934
O2	$\frac{1}{2}$, 0, 0.3785	1.003	$\frac{1}{2}$, 0, 0.3786	1.001
O3	0, $\frac{1}{2}$, 0.3780	1.010	0, $\frac{1}{2}$, 0.3779	1.002
O4	0, 0, 0.15845	0.982	0, 0, 0.15865	0.987

traction was done both in real space and in reciprocal space in which case the $S(Q)$'s were subtracted, and the results were identical.

The Rietveld refinement of the neutron diffraction pattern confirmed the known crystal structure symmetry[25] and provided the atom parameters and unit cell dimensions. The refinement of the occupancies yielded an oxygen content of about 6.92 ± 0.02 for both the ^{63}Cu and ^{65}Cu-YBCO samples. The thermal factors show small differences between the two samples. Some of the results of the refinement are summarized in Table I. A model PDF can be calculated from the atomic coordinates and unit cell dimensions defined by the constraints of the *Pmmm* symmetry to provide a one-dimensional function of the atomic pair distance correlations. The model PDF for the local structure is constructed in the following way:

$$\rho(r)_{\mathrm{mod}} = \sum_{i,j} c_i c_j \frac{b_i b_j}{\langle b \rangle^2} \delta(r_i - r_j) e^{(r_i - r_j)^2 / 2\sigma^2}, \qquad (5)$$

where c_i is the concentration of atom i in the unit cell. The δ functions correspond to distances in real space separating two atoms. They are convoluted by a Gaussian function which broadens the peak width simulating quantum zero-point motion and thermal vibrations. The peak width σ is refined to best fit the experimental peak widths. The model for the local structure with input parameters obtained from the Reitveld refinement is shown in Fig. 2(a) and 2(b) (solid line) and is compared to the experimentally determined PDF's for the ^{65}Cu-YBCO and ^{63}Cu-YBCO compounds at 112 K (symbols). The agreement between the model and experiment is quite good as can be seen up to 8 Å. This can be additionally quantified by the agreement factor A defined by

$$A = \left[\frac{\int_{r_1}^{r_2} [\rho_{\mathrm{exp}}(r) - \rho_{\mathrm{mod}}(r)]^2 dr}{[\rho_0 \int_{r_1}^{r_2} dr]^2} \right]^{1/2}, \qquad (6)$$

where ρ_{exp} and ρ_{mod} are the experimental and model PDF's and ρ_0 is the average number density. r_1 and r_2, the limits of integration, are taken from 1.7 to 10 Å. The A factor is a measure of the goodness of fit between the model and experiment, similar to the R factor in the Rietveld refinement. For the model shown in Fig. 2(a), $A = 0.116$. At the same temperature, a comparison of the ^{63}Cu-YBCO compound

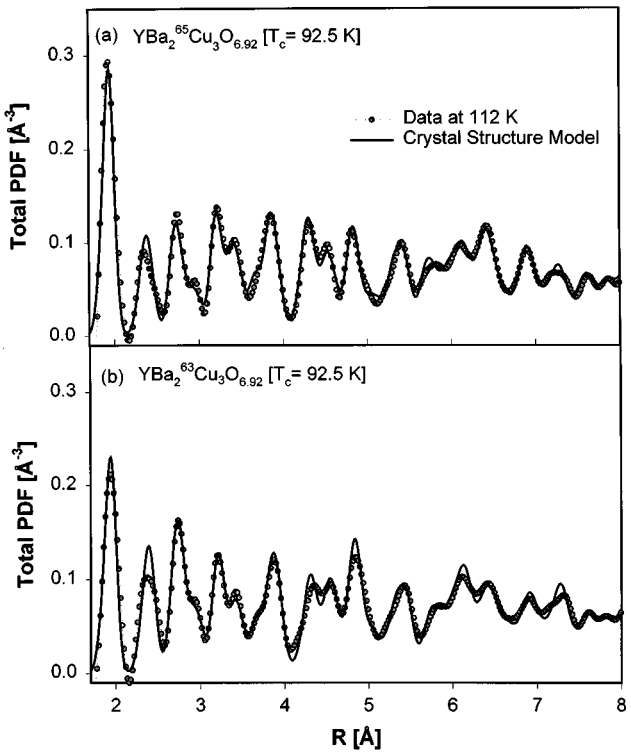

FIG. 2. The experimentally determined PDF of the (a) ^{65}Cu-YBCO and (b) ^{63}Cu-YBCO (solid line) determined at 112 K is compared to a model PDF (symbols) for the average crystal structure with the parameters listed in Table I.

with the model yields an agreement of $A = 0.110$ [Fig. 2(b)]. As can be seen, both samples agree quite well with the already existing crystallographic model. For comparison, the Ni element used as a standard in the analysis provides an agreement factor of $A = 0.180$, with the known fcc model for the Ni crystal.

III. RESULTS AND DISCUSSION

The model PDF's for the atom specific, or partial, PDF's (PPDF) with respect to the two crystallographically distinct types of copper atoms, Cu1 (chain) and Cu2 (plane), are shown in Fig. 3. They provide a local atomic representation with regard to the copper ion alone, enabling the identification of pair correlations at specified distances. The PPDF's include all pair correlations with respect to copper, including the Y and Ba as well as self-correlations. Some of the peaks are labeled including the Cu1-O4 at 1.9 Å and the Cu2-O4 at 2.3 Å peaks. As can be seen, the Cu1-O4 peak is found at the same distance as the Cu1-O1 and the Cu2-O2/O3 correlations. On the other hand, the Cu2-O4 peak as seen in the Cu-PPDF is completely isolated as it does not overlap with any other Cu-O bond. For comparison, this small peak is completely obscured in the total PDF, as the Cu2-O4 bond overlaps with the Y-O2/O3 and the Ba-O pair correlations.

Substraction of the total PDF for ^{63}Cu-YBCO from the ^{63}Cu-YBCO yields the Cu DPDF. The experimental Cu-DPDF determined at 112 K (symbols) is also shown in Fig. 3 and is compared to a model DPDF for Cu (solid line). This model is built using the average crystal structure as the main frame superimposed with some local distortions, and the de-

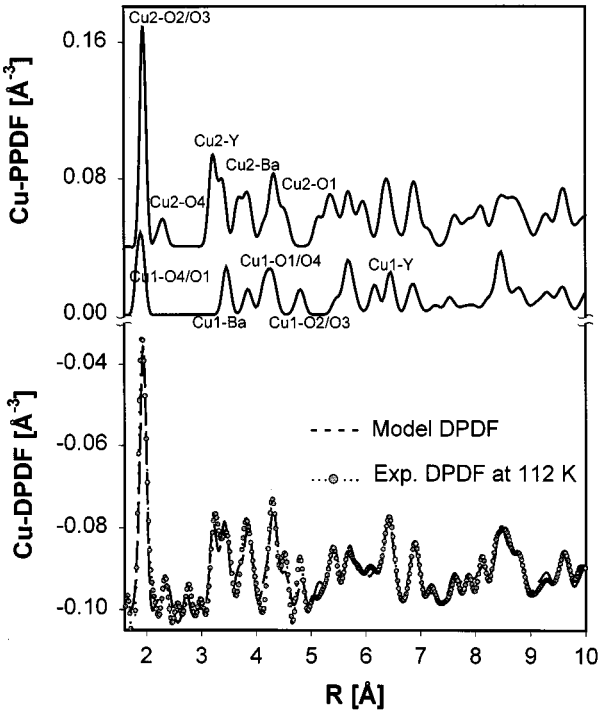

FIG. 3. The PPDF's for Cu1 and Cu2 showing all correlations with respect to copper (solid lines). Also, the Cu-DPDF determined in the normal state at 112 K (symbols) is compared to the model Cu-DPDF (dashed line). Note that the Cu2-O4 peak shows a very small split, if any, at this temperature. The amplitude of the second peak at this temperature is very low, at about the level of noise.

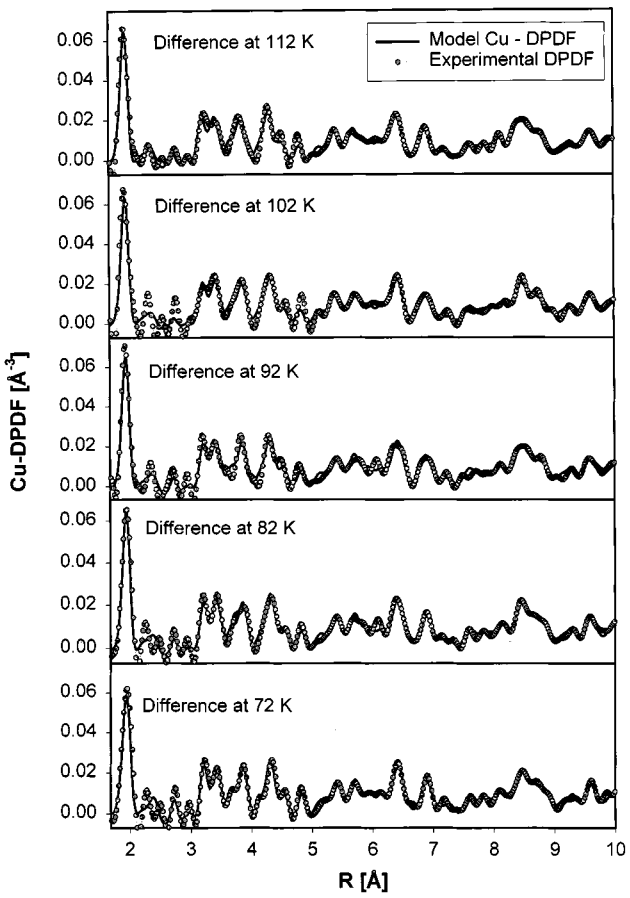

FIG. 4. The Cu DPDF at 112, 102, 92, 82, and 72 K. The data at each temperature are compared to a model for the Cu-DPDF. The agreement between the model and experimentally determined DPDF is quite good at all temperatures but some deviations are observed between 2–3 Å. As can be seen, a split in the Cu2-O4 correlations develops above T_c and it is still present in the superconducting state.

tails will be given further below. The first peak in the DPDF centered around 1.92 Å corresponds to the pair correlations given in Table II as determined from the partials for the two types of copper atoms and includes the Cu1(chain)-O4(apical) bond. The FWHM of this peak is 0.15 Å which is broad and originates from the cumulative sum of all the bond pairs listed in Table II. These pairs vary slightly in their actual bondlength from the average 1.92 Å separation, giving rise to peak broadening. The second peak in the DPDF at 2.3 Å corresponds to the Cu2-O4 pair only. As seen from the top function of Fig. 3, only the Cu2-O4 pair has a correlation with this bond length, making it unique in the DPDF. The amplitude of this peak is considerably smaller than that of the first peak in the function because it consists solely of this one pair, in contrast to the first peak which consists of a total of four different kind of pairs.

From the normal to the superconducting state, the local Cu environment changes as a function of temperature in the way shown in Figs. 4 and 5 (short scale). Significant differences are observed in the local atomic structure corresponding to the Cu2-O4 correlations, as a function of decreasing temperature. While a single Cu2-O4 peak, with a FWHM of ~0.09 Å, is evident in the data at 112 K, by lowering the temperature, this peak splits into two, at ~2.3 and ~2.6 Å. The position of these two peaks shift with temperature however, getting to smaller bond length values at 82 and 72 K. In the expanded scale of Fig. 5, a wiggle is seen in the function at 112 K at 2.6 Å as in the data at 102 K. However, in the former case, the amplitude is small, at the noise level, making it difficult to determine whether this peak is present at 112 K or not. It is possible that as the temperature is raised higher than 112 K, this wiggle goes away, indicating the complete disappearance of the doubling Cu2-O4 correlation. In contrast, the first peak in the PDF shows very little change with decreasing temperature. The width of this peak does not vary significantly with temperature indicating that the Cu1-O4 correlations do not exhibit a noticeable change during the transition process. In addition, by comparing the data above and below T_C, it can clearly be seen that the local atomic structure *at* T_C is quite different than the one above and below. This could suggest coupling of the transition to the lattice.

TABLE II. Pair correlations of copper-oxygen atoms involved at the specified distances. The width of the peaks originates from the spread of the different bondlengths.

Peak~1.9 Å	Peak~2.3 Å
Cu1-O4	(2) Cu2-O4
Cu1-O1	
Cu2-O2	
Cu2-O3	

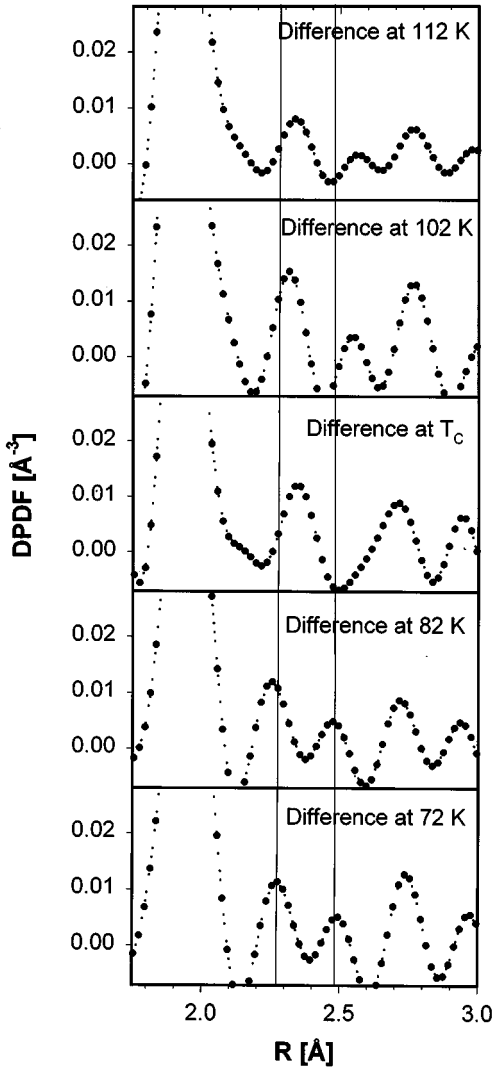

FIG. 5. The Cu DPDF above, at and below T_c at a short scale to amplify the Cu2-O4 correlation region. Note a shift of the Cu2-O4 bonds to lower values in the superconducting phase in contrast to the values in the normal state.

The doubling of the Cu2-O4 pair correlations is additionally observed in the total PDF for the local structure by looking at differences in the PDF's with temperature per isotopic sample, separately. This is done by summing all the PDF's measured above T_C and taking the difference from the summed PDF's measured below (Fig. 6). The data collected at 112 and 102 K are relatively close in temperature and summing them up improves the counting statistics and makes the subtraction more reliable. The same holds true for the data at 82 and 72 K. The same substraction was carried out for both samples and the difference is shown as the black line in the two panels of Fig. 6. In the region of the expected Cu2-O4 peaks, from 2.2–2.5 Å, the difference line is not zero as the Cu2-O4 peaks was shown to shift with temperature above. This provides added confirmation on the presence of this local atomic undulation instigated around the transition.

The data show that the Cu2-O4 pair correlations bifurcate with a separation of about 0.25 Å. However, the absolute magnitude of this separation might not be as reliable because

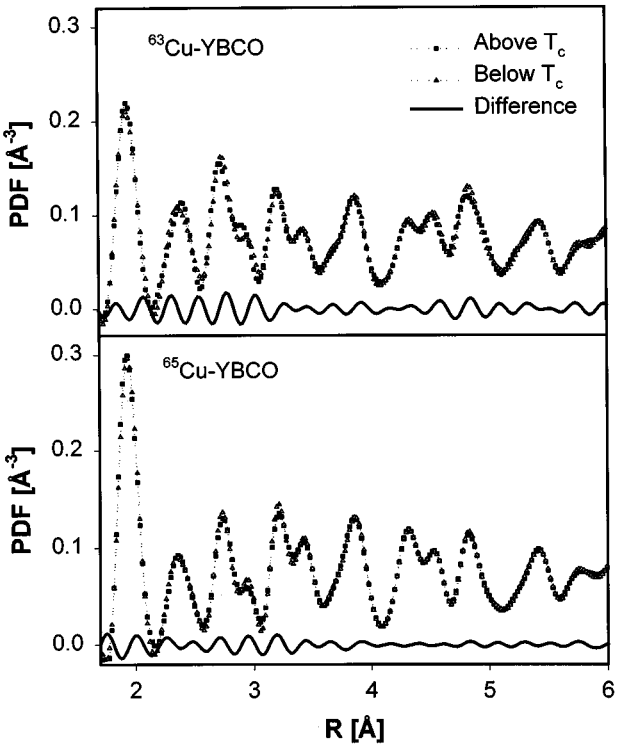

FIG. 6. (top) ^{63}Cu-YBCO, (bottom) ^{65}Cu-YBCO. A difference (solid line) in the total PDF obtained by subtracting the data in the normal state from the data collected in the superconducting state. The split in the Cu2-O4 region is still present as in the DPDF's.

of the limitations in the Fourier truncation and due to a particular dynamic effect of the spectrometer. It can be seen that as the value of $Q_{\max}$ over which the transform is extended varies, the position and separation of the two peaks vary as well (Fig. 7). In the lower limit, for the lowest value of $Q_{\max}=23\,\text{Å}^{-1}$ (dashed line), the resolution between the two peaks is limited and one observes a very broad peak with the weight falling under the more intense peak. In the upper limit, using a higher cutoff of $Q_{\max}$ enables the resolution of the two peaks, but the absolute peak positions shift. Consequently, one can consider that such a double Cu2-O4 peak is present, where $\frac{2}{3}$ of the pairs are close to 2.25 Å and $\frac{1}{3}$ are of a somewhat larger separation. In addition, the lattice distor-

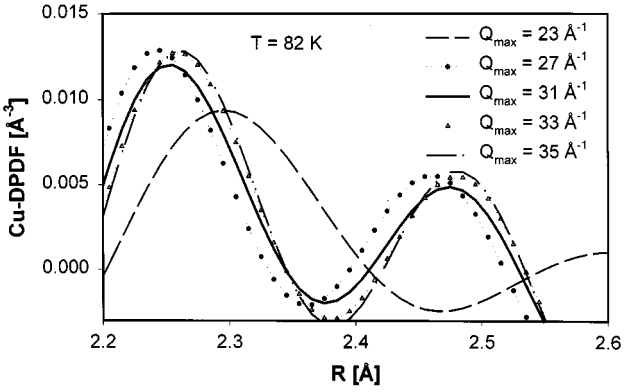

FIG. 7. The dependence of the positions of the Cu2-O4 peaks with the termination Q vector. Reducing the Q cutoff reduces the resolution between the two peaks.

tions induced by displacements of the Cu2-O4 pair might also be dynamic. The $S(Q,\omega)$ at GLAD is integrated over energy, mixing up static and dynamic events if present. In reality however, the integration is limited by the kinematics of the spectrometer giving rise to an energy cutoff. The limited ω_c provides added complications in the determination of PDF in the case where lattice excitations are of the order of ω_c. Distortions can be introduced in the Fourier transform, such as shifts in the peak positions, which are not necessarily real where these shifts depend on the diffraction angle. Details of this phenomenon can be found in Refs. 17, 26 with several examples of other systems showing dynamic lattice effects. Such an effect might be present in this case as well, suggesting that while the two peaks in the PDF are present, their exact separation cannot be well defined.

From Fig. 2, the model PDF for the long range crystal structure compares well with the experimental PDF. However, some small discrepancies between the two are evident which can be minimized through real space refinement. In a similar manner to the Rietveld refinement, the ionic positions are adjusted to reduce the *A* factor. The first part of the model takes into account disorder, localized around defect sites. In the current case, small displacements of atoms are introduced in the vicinity of vacancies found in the chains of the structure. The amplitude of the atomic displacements away from equilibrium is small. As there is about 1% of vacancies in these samples, it is reasonable to assume that some localized deformations centered around the defect sites in the chains can be created. To simulate such a distortion, we assumed small displacements of the chain copper, Cu1, the Ba and the planar oxygen, O2, of 0.1 Å in the *a* direction, 0.05 Å along the *c* axis, and 0.12 Å towards the vacancy, respectively. This improved the model.

Further structural refinement which included distortions of the Cu2 and O4 atoms yield even better results. In this case, the motion appeared to be most favorable if the atoms were displaced along the *c* axis of the crystal but in opposite orientations, by 0.05 Å. These small atomic displacements from their ideal crystallographic sites improved the fit of the model to the data by lowering the *A* factor even further ($A=0.107$ for the ^{65}Cu-YBCO and $A=0.090$ for ^{63}Cu-YBCO with slightly different sigmas for the peak widths). The difference in the *A* factors between the two samples comes mostly from the fact that the PDF peaks of the ^{65}Cu samples are sharper because of its larger scattering amplitude than the ^{63}Cu sample. The resulting PDF for the refined model is shown in Fig. 8. The nature of the atomic distortions in the CuO_2 planes are consistent with other studies of the YBCO system.[27] Displacements other than the ones stated increase the differences between model and experiment. Overall, the outlined distortions contribute to a local inhomogeneity which gives rise to a very good agreement between the model and experiment in the Cu-DPDF as seen from Fig. 3 as well as in the total PDF (Fig. 8). Further modeling is required however to reproduce the temperature dependence of the split in the Cu2-O4 correlations as seen experimentally. In the current distorted Cu-DPDF model (solid lines, Figs. 3 and 4), a number of Cu2-O4 pairs have short bonds at 2.21 Å in addition to the pairs with average separation of 2.315 Å. This does indeed provide a split in the Cu2-O4 correlations in the model as well, but the details still need further attention.

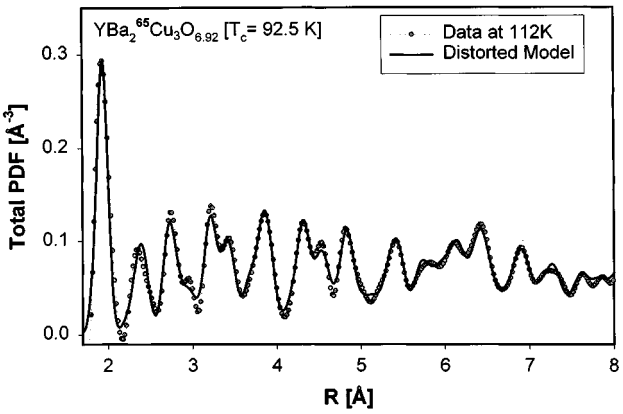

FIG. 8. The experimentally determined PDF at 112 K (symbols) is compared to a distorted model for the crystal structure. This model includes distortions of the Cu2-O4 pair along the *c* axis of the crystal, in addition to some displacements around the vacancies which involve the Cu1, Ba, and O2 atoms.

If a split in the Cu1-O4 bonds of the order of 0.135 Å develops in the superconducting state, the width of the first peak in the experimental PDF would almost double and the height would come down. This is not what is observed, however. In addition, from the above distorted model for the local structure, it can be deduced that two types of Cu1-O4 bonds are likely to be present locally, one at 1.845 Å and another at 1.872 Å. This difference in the Cu1-O4 interatomic distance (0.027 Å) is *considerably* less than the suggested value of 0.135 Å by XAFS studies. For comparison, the crystallographic model provides only one type of Cu1-O4 bond, at 1.845 Å. But with the above distorted model, it has been possible to introduce a number of sites with a somewhat longer Cu1-O4 bond which is still not far from the average value. However, the current model cannot accommodate distortions as large as the ones suggested by XAFS studies.[4]

It is quite unexpected to observe local distortions associated with the Cu2-O4 peak and not the Cu2-O4 pair, since both coppers are bonded to the same O4 atom. This serves as a clear indication that such a lattice distortion most likely results from displacements of the copper atoms found in the planes. If the oxygen atoms, O4, were driving the distortions, one would have expected both peaks involving Cu1-O4 (1.92 Å) and Cu2-O4 (2.25 Å) pairs to change. That is, if the source of the distortions was the O4 atoms correlations changing in going from the normal to the superconducting state, both of these peaks would have exhibited some temperature variation (Figs. 4 and 5). This is not the case, however. The separation proposed previously[4] of 0.135 Å of the Cu1-O4 bonds is substantial which would have been easily identified with the technique used in this study. This means that in reality, the O4 atom does not exhibit any uncharacteristic displacements from its ideal position and this is additionally confirmed by our Rietveld thermal factors for O4 which are very small and spherically symmetric. This leads to the conclusion that any observed chain lattice effects arise partly from static distortions which exhibit some temperature dependence but do not appear to be linked to the proposed

mechanism of charge transfer from the chains to the superconducting planes. On the other hand, more pronounced lattice effects appear to be linked with distortions of the planar copper atoms. One would expect that the motion of Cu2 would also distort the Cu2-O2/O3 correlations. However, in the extreme case of a Cu2 displacement of 0.2 Å, the Cu2-O2/O3 bonds would change by 0.01 Å which is barely noticeable if the motion were perpendicular to the plane. But in the case where the displaced motion were parallel to the plane then the Cu2-O2/O3 bonds would change significantly. Thus, the direction of distortion of the Cu2 ions has to be along the *c* axis of the crystal.

In conclusion, we studied the local atomic structure of the YBCO superconductor to investigate the nature of the lattice effects during the phase transformation. This is a successful use of the isotope DPDF technique for a superconductor. Evidence for the coupling of the local lattice effects to the superconducting transition in this system is provided. Possible copper displacements in the superconducting planes are the cause of the double Cu2-O4 interatomic distance correlations in the vicinity of T_C.

ACKNOWLEDGMENTS

The authors would like to acknowledge many valuable discussions with T. Egami, P. C. Hammel, H. Röder, A. Bussman-Holder, and C. H. Booth. Work at the Los Alamos National Laboratory is performed under the auspices of the U.S. Department of Energy under Contract No. W-7405-Eng-36. The IPNS is supported by the U.S. Department of Energy, Division of Materials Sciences, under Contract No. W-31-109-Eng-38. B.D. and Z.B. were supported by the National Science Foundation, Science and Technology Center for Superconductivity under Contract No. DMR-91-20000.

[1] For a review see *High Temperature Superconductivity*, edited by K. S. Bedell, D. Coffey, D. E. Meltzer, D. Pines, and J. R. Schrieffer (1989), in *Lattice Effects in High T_c Superconductors*, edited by Y. Bar-Yam, T. Egami, J. Mustre de Leon, and A. R. Bishop (World Scientific, Singapore, 1992).

[2] J. D. Jorgensen, M. A. Beno, D. G. Hinks, L. Soderholm, K. J. Volin, R. L. Hitterman, J. D. Grace, I. K. Schuller, C. U. Segre, K. Zhang, and M. S. Kleefisch, Phys. Rev. B **36**, 3608 (1987).

[3] S. D. Conradson and I. D. Raistrick, Science **243**, 1340 (1989); S. D. Conradson, I. D. Raistrick, and A. R. Bishop, *ibid.* **248**, 1394 (1990).

[4] J. Mustre de Leon, S. D. Conradson, I. Batistic, and A. R. Bishop, Phys. Rev. Lett. **65**, 1675 (1990).

[5] E. A. Stern, M. Qian, Y. Yacoby, S. M. Heald, and H. Maeda, *Lattice Effects in High T_c Superconductors* (Ref. 1), p. 51.

[6] C. H. Booth, F. Bridges, J. B. Boyce, T. Claeson, B. M. Lairson, R. Liang, and D. A. Bonn, Phys. Rev. B **54**, 9542 (1996).

[7] J. Röhler, A. Larisch, and R. Schäfer, Physica C **191**, 57 (1992); J. Röhler, *Materials and Crystallographic Aspects of HT_c-Superconductivity*, edited by E. Kaldis (Kluwer, Dordrecht, 1993), p. 353.

[8] P. Schweiss, R. Reichardt, M. Braden, G. Collin, G. Heger, H. Claus, and A. Erb, Phys. Rev. B **49**, 1387 (1994).

[9] J. D. Sullivan, P. Bordet, M. Marezio, K. Takenaka, and S. Uchida, Phys. Rev. B **48**, R10 638 (1993).

[10] G. H. Kwei, A. C. Larson, W. L. Hults, and J. L. Smith, Physica C **169**, 217 (1990).

[11] G. Roth, B. Renker, G. Heger, M. Herview, B. Domenges, and B. Raveau, Z. Phys. B **69**, 53 (1987).

[12] H. F. Poulsen, N. H. Andersen, J. V. Andersen, H. Bohr, and O. G. Mouritsen, Nature (London) **349**, 594 (1991).

[13] A. W. Hewat, J. J. Capponi, C. Chaillout, M. Marezio, and E. A. Hewat, Solid State Commun. **64**, 301 (1987).

[14] T. Zeiske, D. Hohlwein, R. Sonntag, J. Grybos, K. Eichhorn, and T. Wolf, Physica C **207**, 333 (1993).

[15] T. Egami and S. J. L. Billinge, *Progress in Materials Science* (Elsevier, London, 1994), Vol. 38, p. 359; T. Egami and S. J. L. Billinge, *Physical Properties of High Temperature Superconductors V*, edited by D. M. Ginsberg (World Scientific, Singapore, 1996), and references therein.

[16] B. H. Toby, T. Egami, J. D. Jorgensen, and M. A. Subramanian. Phys. Rev. Lett. **64**, 2414 (1990); T. Egami, B. H. Toby, S. J. L. Billinge, H. D. Rosenfeld, J. D. Jorgensen, D. G. Hinks, B. Dabrowski, M. A. Subramanian, M. K. Crawford, W. E. Farneth, and E. M. McCarron, Physica C **185-189**, 867 (1991); W. Dmowski, B. H. Toby, T. Egami, M. A. Subramanian, J. Gopalakrishnan, and A. W. Sleight, Phys. Rev. Lett. **61**, 2608 (1988).

[17] T. Egami, *Materials and Crystallographic Aspects of HT_c-Superconductivity* (Ref. 7), p. 45.

[18] T. Egami, T. R. Sendyka, W. Dmowski, D. Louca, H. Yamauchi, S. Tanaka, and M. Arai, Physica C **235-240**, 1229 (1994).

[19] T. Egami, W. Dmowski, R. J. McQueeney, M. Arai, N. Seiji, and H. Yamauchi, J. Supercond. **8**, 587 (1995).

[20] V. Sears, Neutron News **3**, 29 (1992).

[21] B. H. Toby and T. Egami, Acta Crystallogr., Sect. A: Found. Crystallogr. **48**, 336 (1992).

[22] A. K. Soper, W. S. Howells, and A. C. Hannon, *ATLAS, Analysis of Time-of-Flight Diffraction Data from Liquid and Amorphous Samples* (Rutherford Appleton Laboratory, Chilton, 1989).

[23] G. L. Squires, *Introduction to the Theory of Thermal Neutron Scattering* (Dover, Mineola, NY, 1996), p. 35.

[24] G. H. Kwei, D. Louca, S. J. L. Billinge, and H. D. Rosenfeld, in *Local Structure from Diffraction*, edited by M. F. Thorpe and S. J. L. Billinge (Plenum, New York, 1999), p. 323.

[25] M. A. Beno, L. Soderholm, D. W. Capone, D. G. Hinks, J. D. Jorgensen, J. D. Grace, I. K. Schuller, C. U. Segre, and K. Zhang, Appl. Phys. Lett. **51**, 57 (1987).

[26] D. Louca and T. Egami, Phys. Rev. B **59**, 6193 (1999).

[27] J. Röhler, P. W. Loeffen, K. Conder, and E. Kaldis, Physica C **282-287**, 182 (1997).